Design, Synthesis, and Biological Evaluation of 3,4-Diarylmaleimides as Angiogenesis Inhibitors

Christian Peifer,[||] Thomas Stoiber,[⊥] Eberhard Unger,[⊥] Frank Totzke,[†] Christoph Schächtele,[†] Dieter Marmé,[†] Ruth Brenk,[‡] Gerhard Klebe,[‡] Dieter Schollmeyer,[§] and Gerd Dannhardt*,[||]

Department of Pharmacy, Johannes Gutenberg-University, Staudingerweg 5, D-55099 Mainz, Germany, Department of Single Cell and Single Molecule Techniques, Institute of Molecular Biotechnology, Beutenbergstraβe 11, D-07745 Jena, Germany, ProQinase GmbH, Breisacherstrasse 117, D-79106 Freiburg, Germany, Department of Pharmacy, Philipps-University, Marbacherweg 6, D-35032 Marburg, Germany, and Department of Organic Chemistry, Johannes Gutenberg-University, Duesbergweg 10-14, D-55099 Mainz, Germany

Received May 20, 2005

The new analogue **2** of combretastatin A-4 was discovered to be an inhibitor of tubulin polymerization with an IC_{50} of 7.6 μM and reduced angiogenesis in the in vivo chick embryo model. Interestingly, in a series of 2,3-diarylmaleimides closely related to this lead, no other compound was found to be active in the tubulin polymerization assay. However, by screening in the in vivo chick embryo assay **10** was identified as a potent angiogenesis inhibitor indicating an alternative target. Indeed, molecular modeling studies suggest a reasonable binding mode of **10** at the ATP-binding site of the model kinase CDK2. Motivated by these results, analogues of **10** were screened for inhibitory activity in a panel of 12 selected protein kinases and a high affinity of **10** to VEGF-R2 was found showing an IC_{50} of 2.5 nM. Structure−activity relationships (SAR) for this compound series with the isolated enzyme and equivalent antiangiogenic activity in the chick embryo assay are presented herein.

Introduction

A number of pathological events such as solid tumor growth and metastasis but also several nonmalignant diseases such as macular degeneration, arthritis, or psoriasis in humans have been found to be associated with angiogenesis, the formation of new blood vessels from preexisting vasculature.[1] Concerning the neoplastic field, an innovative approach in the treatment of diseases consists of blocking or delaying the progression of neovascularization to dysplastic cells to stop the delivery of nutrition and oxygen. Since physiological angiogenesis in adults is strictly limited, compounds with antiangiogenic activity may be useful to treat cancer with potentially less systemic toxicity than conventional cytotoxic therapeutics.[2] Furthermore, tumor vessels can be distinguished from normal physiological vasculature by their immature development and chaotic architecture due to a serious disorder of the angiogenic process.[3] In contrast to the antiangiogenic approach, targeting the established vessels to cause a rapid shutdown of vasculature leading to secondary tumor cell death is referred to as the antivascular approach.[4] A promising antivascular concept to interfere selectively with recently built capillaries is to target the microtubule system of endothelial cells with tubulin binders. Natural tubulin binders are colchicine, the vinca alkaloids, rhizocin, maytensine, combretastatins, epothilone, and the taxanes.[5] These agents generally exert their effects by microtubule depolymerization or stabilization and some belong to one of the most effective classes of drugs in clinical use for anticancer treatment. One interesting group among the diverse tubulin polymerization inhibitors are the combretastatins, natural products isolated from the South African tree *Combretum caffrum*. Studies showed combretastatin stilbene derivatives to be members of the colchicine-like inhibitors with extraordinary affinity for the tubulin system.[6] Selected for preclinical development was combretastatin A-4 (CA-4) (**I**, Chart 1). Its prodrug combretastatin A-4 disodium phosphate causes a virtually complete vascular shutdown in several tumors within minutes after administration. [7] Because of the relatively simple structure and the strong potency against a broad spectrum of human cancer cell lines, CA-4 is a very attractive lead compound. Thus, a large number of modifications and analogues have been synthesized, and structure−activity relationships were described.[8,9] Since only the cis isomer possesses strong antitubulin activity but it tends to isomerize to the inactive trans isomer,[10] a ratio was to place the cis double bond in an additional ring system to arrest the cis conformation resulting in a noncoplanar orientation of the two aromatic rings (e.g., in Chart 1, 1,3-imidazole **II**, 4,5-imidazole **III**, and oxazole **IV** derivatives).[11] A similar approach resulted in the antimitotic (*S*,*S*)-isomer of combretadioxolan (**V**, Chart 1)[12] and also diarylindoles (**VI**, Chart 1) fulfilling this concept successfully.[13] Recently, investigations on pyridine derivatives (**VII**, Chart 1) and *cis*-4,5-diphenylisoxazolines (**VIII**, Chart 1) of CA-4 have been reported.[14] A number of these structural enhancements were found to be well tolerated, and compounds with comparable activity to CA-4 were described.

In this study, we report the synthesis and biological evaluation of the new CA-4 analogue 3-(3,4,5-trimethoxyphenyl)-4-(3-hydroxy-4-methoxyphenyl)-1*H*-pyrrole-2,5-dione **2** (Figure 1) and related compounds bearing the maleimide (1*H*-pyrrole-2,5-dione) moiety as a core structure. The maleimide element occurs as a structural part in several natural compounds, for example, the antitumor indolocarbazole rebeccamycin[15] (**IX**, Chart 2), a topoisomerase-I inhibitor. Chemically related to rebeccamycin, staurosporine (**X**, Chart 2) represents another indolocarbazole with broad and potent activity against several kinases at the ATP site (e.g., cyclin-dependent kinase 1 (CDK1), IC_{50} = 4 nM).[16] Derived from the unselective structural lead staurosporine, 2,3-diarylmaleimides have been designed and described as protein kinase inhibitors (e.g., protein kinase C (PKC) inhibitor bisindolylmaleimide **XI**, Chart 2, PKC IC_{50} = 0.11 μM)[17] or glycogen synthase kinase-3 inhibitors[18]).

* To whom correspondence should be addressed. Tel: +49 6131 39-25728. Fax: +49 6131 39-23062. E-mail: dannhardt@uni-mainz.de.
[||] Department of Pharmacy, Johannes Gutenberg-University.
[⊥] Institute of Molecular Biotechnology.
[†] ProQinase GmbH.
[‡] Philipps-University.
[§] Department of Organic Chemistry, Johannes Gutenberg-University.

10.1021/jm0580297 CCC: $33.50 © 2006 American Chemical Society
Published on Web 02/02/2006

Chart 1. Combretastatin A-4 (CA-4, **I**) and Antimitotic 1,2-Substituted Five-Membered Heterocycle Derivatives (**II**−**VIII**) Showing the Same Aromatic Substitution Pattern

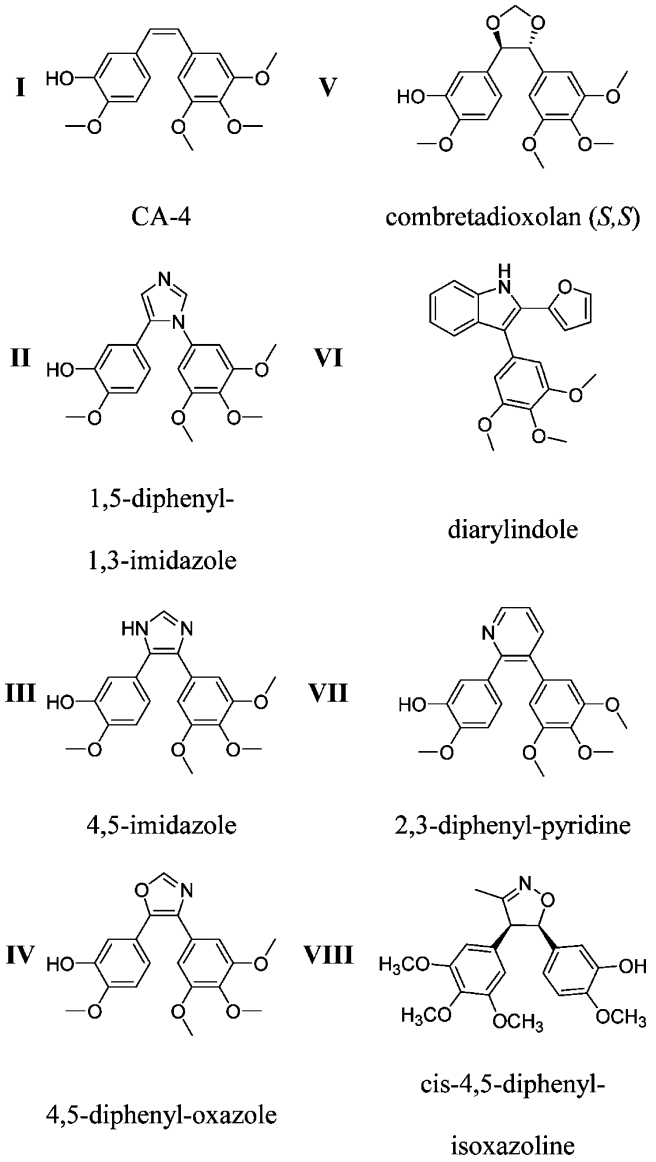

To prove the concept of combining CA-4 and maleimide, compound **2** and closely related analogues were synthesized and evaluated for their biological activity. By screening 2,3-maleimides for antiangiogenic activity in the in vivo chick embryo assay, we identified some of the new compounds as potent angiogenesis inhibitors. In the present paper, structure−activity relationships (SAR), as well as biological properties, of selected 2,3-diarylmaleimides are presented.

Results and Discussion

Synthesis of Asymmetrical 3,4-Diarylmaleimide Derivatives. Among the number of synthetic methods for preparing 3,4-diarylmaleimides, the method of Faul et al. can be used conveniently. According to the procedure, asymmetrically substituted 3,4-diarylmaleimides were prepared by one-pot ligand condensation of arylacetamide units with aryl glyoxylethyl esters using KOBu^t in THF (Scheme 1). [19] This approach has been reported to be efficient concerning the toleration of various functional groups and provides good yields. In the present study, we used 0.1 M KOBu^t in BuOH and additionally 4 Å mol sieves to bind the water generated in the chemical

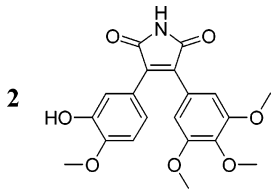

Figure 1. Structure of 3-(3,4,5-trimethoxyphenyl)-4-(3-hydroxy-4-methoxyphenyl)-1*H*-pyrrole-2,5-dione (**2**).

Chart 2. Natural Compounds Rebeccamycin (**IX**, Bearing the Maleimide Moiety), Staurosporine (**X**, 1,5-Dihydro-pyrrol-2-one), and Related Bisindolylmaleimide (**XI**)

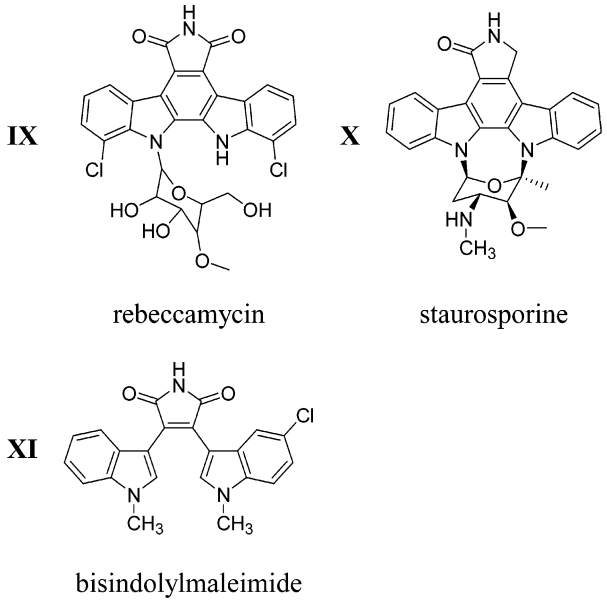

reaction. The arylacetamides were readily available via amidolysis of the commercially available aryl acetyl chlorides. Aryl glyoxylethyl esters were synthesized by Grignard reaction (**3**[20] for preparation of compounds **4** and **9**) or obtained via Friedel−Crafts-type acylation of the desired aryl derivatives with methyl or ethyl oxalyl chloride (**1**,[21] 3-indole derivatives for preparation of compounds **10**, **10a**, **12**, **12a**, **13**, **14**, **15**, **16**, **16a**, **18**, **19**, and **20**,[22] ethyl-(1-methylindolyl-3)-glyoxylate[19b] for preparation of compound **17**,[23] 1*H*-pyrrole-3-ethylglyoxylate for preparation of compound **11**,[24] and indole-2-ethylglyoxylate for preparation of compound **21**,[25] Tables 1−3). According to this concept, the aim was to prepare 3-hydroxy-4-methoxyphenyl methylglyoxylate as a key precursor for the synthesis of the CA-4 analogue 3-(3,4,5-trimethoxyphenyl)-4-(3-hydroxy-4-methoxyphenyl)-maleimide (**2**). To address this goal, we started from guajacol (as schown in Scheme 2). 5-Substituted guajacol derivatives are difficult to prepare since the electrophilic substitution of guajacol takes place predominantly at the 4-position while the corresponding mesylate (masking the phenol into a deactivating group) directs the entry to the 5-position.[21] We found out that it was not necessary to remove the mesylate from **1** prior to the formation of the maleimide by reaction with 3,4,5-trimethoxyphenyl acetamide: when 4 equiv of KOBu^t were used to remove the mesyl group in the reaction simultaneously, compound **2** (bearing the free phenolic function) was obtained in moderate yield (44%). The structure of **2** was proven by X-ray analysis (see experimental data, Figure 2).

In solution, compound **10** was found to be chemically instable by generating the corresponding carbazole **10a**. The structures of **10** and **10a** were proven by X-ray analysis (see experimental data, Figure 3).

Scheme 1. Synthesis of the Maleimide Moiety by Using the Method of Faul et al.[a]

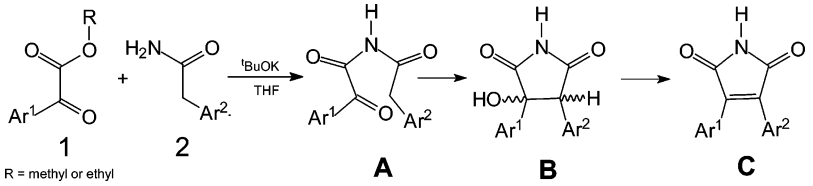

[a] The reaction mechanism is discussed as follows:[19] By addition of KOBu^t into a stirred solution of arylglyoxylylester **1** and arylacetamide **2** in THF, the amide is acylated yielding the tricarbonyl intermediate **A**, which undergoes an intramolecular Perkin-type condensation to hydroxy imide **B**. Using an excess of KOBu^t (2−4 equiv) causes dehydration to maleimide **C** via an E2 or E1CB mechanism. Molecular sieves (4 Å) was used to bind the water generated in the chemical reaction.

Table 1. Tubulin Inhibitory Activity and Inhibition of Vessel Growth in the in Vivo Chick Embryo Model of 3,4-Diarylmaleimides **2**−**11** (Series A) Bearing Core Structure **A**

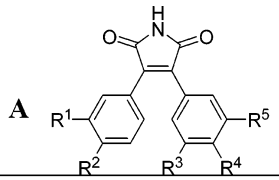

cpd.	R^1	R^2	R^3	R^4	R^5	ITP[a] IC_{50} (μM)	IVG[b] (% inh.)	μg
CA-4						2.1[c]	-[d]	0.5
2	OH	OCH_3	OCH_3	OCH_3	OCH_3	7.6	76.9	10
4	H	OCH_3	OCH_3	OCH_3	OCH_3	NE[e]	27.3	10
5	H	H	OCH_3	OCH_3	OCH_3	NE	32.2	50
6	H	H	H	OCH_3	OCH_3	NE	2.8	50
7	H	H	H	OCH_3	H	NE	16.4	50
8	H	H	H	H	H	NE	11.3	50
9	H	OCH_3	H	OCH_3	H	NE	47.4	10
10	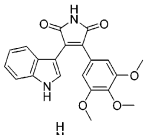					NE	81.7	10
11	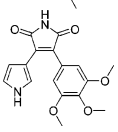					NE	47.2	20

[a] Inhibition of tubulin polymerization. [b] Inhibition of vessel growth versus control in the chick embryo assay after incubation hour 24. Each experiment was performed with 15 samples. [c] Data from ref 6. [d] Determination not possible due to high toxicity of CA-4; all embryos died within 2 h. [e] NE = no effect was observed at a concentration up to 10 μM.

Carbazole Derivatives. Indolocarbazole alkaloids are a very interesting class of natural products. The most well-known members of this family are rebeccamycin and staurosporine owing to their wide range of pharmacological activities. The indolocarbazole, the common aglycon moiety of these compounds, is known to retain much of the activity of the parent molecules.[26] Several methods have been reported for the synthesis of carbazoles, among them an approach involving oxidative cyclization of diindolylmaleimides[27] and 3-aryl-4-indolylmaleimides.[28] Since in these studies several bisarylmaleimides have been reported to readily undergo oxidative cyclization, we supposed an analogous mechanism for 3,4-diarylmaleimides synthesized in the present approach. However, carbazole derivatives **10a** (structure proven by X-ray analysis), **12a**, **16a**, and **17a** (Table 3) were isolated by chromatography from the reactions leading to the corresponding 3,4-diarylmaleimides. Although no further investigations in terms of mechanistic aspects were carried out, in analogy to the reported reaction mechanism,[27,28] the formation of carbazoles is discussed herein as oxidative cyclization of several 3-aryl-4-indolylmaleimides as shown in Scheme 3.

Biological Evaluation. To prove the concept of combining CA-4 and the maleimide moiety, compound **2** was synthesized and evaluated for antimitotic potency. It was found to be active in the in vitro tubulin-assembly assay, and an IC_{50} of 7.6 μM was determined (Table 1; in comparison, the IC_{50} for CA-4 was reported to range from 0.53 to 3.0 μM[11]). The antiangiogenic activity of **2** in the in vivo chick embryo model revealed 76.9% inhibition of vessel area by application of 10 μg per pellet (Table 1). Motivated by these results, a small series of analogues closely related to this concept was prepared under maintenance of the 3,4-diarylmaleimide moiety (series A with core structure **A**; Table 1). Interestingly, none of these compounds was active in the tubulin assembly assay. However, by screening series A for antiangiogenic activity, we identified compound **10** with strong potency against vessel growth in the in vivo chick embryo assay (81.7% inhibition of vessel area after 24 h incubation by application of 10 μg per pellet, Table 1). HPLC analysis of the

Table 2. Inhibition of Vessel Growth in the in Vivo Chick Embryo Model of 3-Aryl-4-indolylmaleimides **10**−**19** (series B) Bearing Core Structure **B** and of **20** and **21**

B

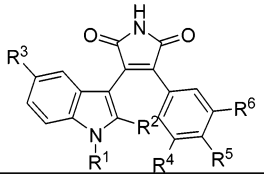

cpd.	R^1	R^2	R^3	R^4	R^5	R^6	IVG[a] (% inh.)	µg
10	H	H	H	OCH_3	OCH_3	OCH_3	81.7	10
12	H	H	H	H	H	H	21.3	10
13	H	H	H	H	OCH_3	H	19.4	10
14	H	H	H	H	OCH_3	OCH_3	71.8	20
15	H	H	H	H	Cl	H	35.2	10
16	H	H	OCH_3	OCH_3	OCH_3	OCH_3	14.4	10
17	CH_3	H	H	OCH_3	OCH_3	OCH_3	23.5	10
18	H	CH_3	H	OCH_3	OCH_3	OCH_3	41.0	25
19	H	C_6H_5	H	OCH_3	OCH_3	OCH_3	37.6	20
20			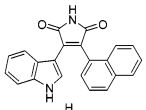				15.2	10
21			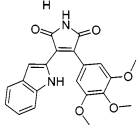				71.1	10

[a] Inhibition of vessel growth versus control in the chick embryo assay after incubation hour 24. Each experiment was performed with 15 samples.

Table 3. Inhibition of Vessel Growth in the in Vivo Chick Embryo Model of Carbazole Derivatives Generated by Oxidative Electrocyclization of the Corresponding 3-Aryl-4-indolylmaleimides

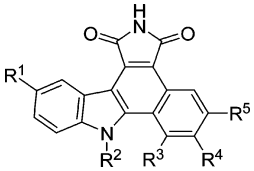

compd	R^1	R^2	R^3	R^4	R^5	IVG[b] (% inh)	amt (µg)
10a	H	H	OCH_3	OCH_3	OCH_3	10.7	10
12a	H	H	H	H	H		
16a	OCH_3	H	OCH_3	OCH_3	OCH_3	22.9	10
17a	H	CH_3	OCH_3	OCH_3	OCH_3		

content uniformity in the production process of agarose pellets (ideal value containing 10 µg of **10**) revealed that the calculated amount per pellet is approximately recovered and that the bulk is homogeneous but that approximately 10% of compound **10a** can be found (Figure 4). Since **10** was applied with analytical purity, the carbazole **10a** was supposed to be generated during the production process of the pellets by oxidative cyclization (as described above, Scheme 3). Investigation of the content of **10** and **10a** in pellet samples by HPLC during the antiangiogenic experiment (Figure 5) indicates only a release of small amounts in 24 h of **10** (0.26 µg) and **10a** (0.02 µg) resulting in the remarkable in vivo effect. When solely **10a** (chemically stable) was investigated in the chick embryo model, 10.7% inhibition of vessel growth by application of 10 µg could be determined in 24 h (Table 3). These findings lead to the conclusion that the biological effects were mainly due to the activity of compound **10**. But without the expected activity against the microtubule system, the significant inhibition of vessel growth suggests an alternative biological target of **10** than that for the lead compound **2**. These results underline the importance of the modified in vivo chick embryo assay used in our investigations. The model can be considered suitable for functional screening of antiangiogenic compounds, as well as to deliver data of biological relevance. Since compound **10** is related to staurosporine and 2,3-diarylmaleimides, which are active against PKC (and other kinases),[17] we hypothesized that **10** was also active against kinases involved in the angiogenic process resulting in the in vivo activity.

Scheme 2. Synthesis of the Key Precursor **1** and Subsequent Formation of **2**[a]

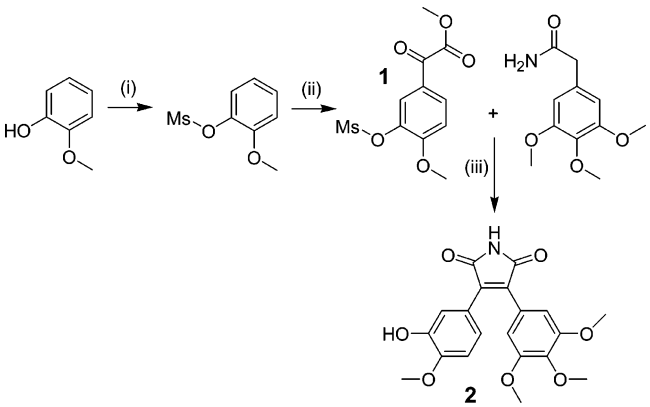

[a] (i) MsCl, TEA; (ii) methylglyoxalate acid chloride, CH_2Cl_2; (iii) 4 equiv of $KOBu^t$ following the general procedure.

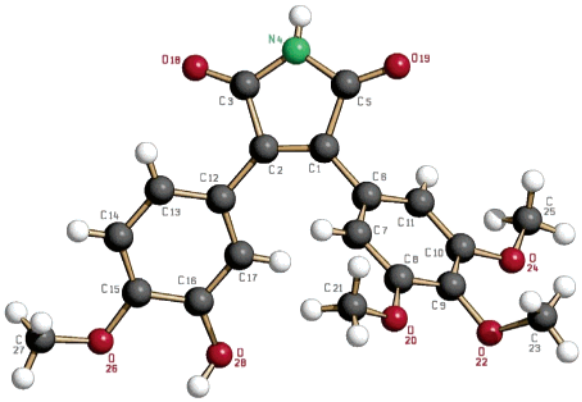

Figure 2. ORTEP molecular structure of compound **2** with the numbering scheme.

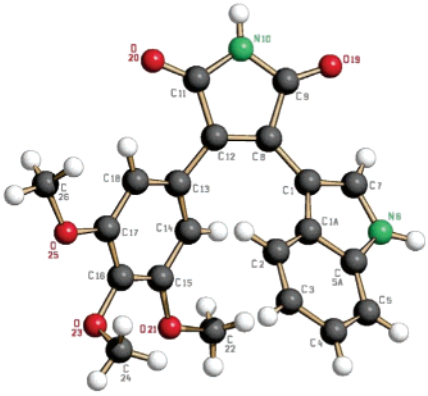

10

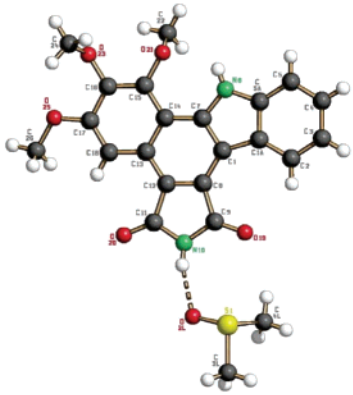

10a

Figure 3. ORTEP molecular structures of compounds **10** and **10a** (containing 1 equiv of DMSO H-bonded to the imide) with the numbering scheme.

Molecular Modeling. To confirm our hypothesis, molecular modeling studies were performed at the ATP binding pocket of CDK2 as model kinase. Even if all members of the kinase family bind the same cofactor, there are slight differences in this pocket and the adjacent subpockets, which can be explored

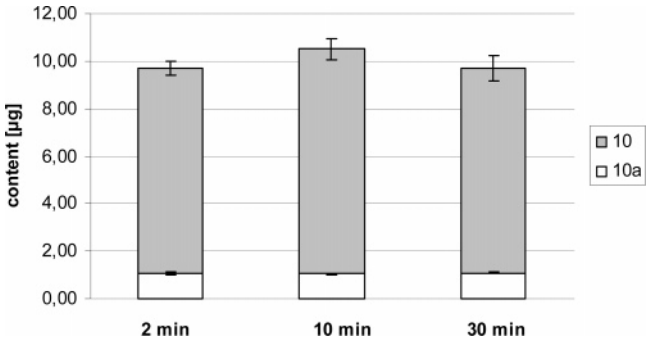

Figure 4. Content of compounds **10** and **10a** in agarose pellets in production process. Each point represents the mean ± SD ($n = 9$).

by ligands.[29] CDK2 in particular was supposed to serve as a valid example because by X-ray crystallography molecular details of the ATP pocket had been well characterized. Furthermore, knowledge of the structure of CDK2 has been a key element in driving the design and development of a large number of ATP competitive inhibitors for which several CDK2-inhibitor structures have been determined. [30] The crystal structure of staurosporine in complex with CDK2 [31] provides insight into the interactions responsible for high-affinity binding to a variety of kinases. Many of these interactions are also observed in other CDK2-inhibitor complexes. Namely, staurosporine forms a hydrogen bond between the lactam nitrogen and the carbonyl oxygen of Glu81. Further the carbonyl oxygen of the lactam moiety is a hydrogen bond acceptor for the backbone amine of Leu83. The extended indolocarbazole ring system is accommodated in the hydrophobic cleft formed by the amino acids Ile10, Val18, Val64, Phe80, Leu134, and Ala144. The glycosyl moiety forms a salt bridge to the carboxylate group of Asp86 via the protonated *N*-methyl amino group and a charge-assisted hydrogen bond to the carbonyl oxygen of Gln131 in the ribose-binding site (Figures 6 and 7).

Docking **10** and **10a** into the binding site with the program FlexX [32] suggests a reasonable binding mode in the ATP-binding pocket of CDK2 (Figures 6 and 7). This binding mode is very similar to the staurosporine binding mode. Likewise, hydrogen bonds to the backbone carbonyl of Glu81 and to the backbone amine of Leu83 are formed. The indole ring and the trimethoxyphenyl moiety are located in the hydrophobic cleft. Although sharing the most important interactions of staurosporine, **10** or **10a** does not address the sugar pocket. This is also the case for numerous other ligands. Even then, they achieve affinities in the micromolar and submicromolar range. [33] Therefore without addressing Asp86 and Gln131 in the sugar pocket, **10** and **10a** are likely to inhibit this kinase. This prompted us to synthesize a series of analogues of **10** (series B, 3-aryl-4-indolyl-derivatives, core structure **B**, Table 2) and **10a** (Table 3) and subsequently to screen these compounds for inhibitory activity in a panel of selected protein kinases.

Kinase Assays. To profile the compounds, 12 kinases were selected for an initial screening. Members of the CDK family (CDK2/cyclinE, CDK1/cyclinB, CDK4/cyclinD1, CDK6/cyclinD1) were chosen because of the molecular modeling data.

Scheme 3. 1,6-π-Electrocyclization of **10** and Subsequent Oxidation of the Intermediate to the Carbazole Derivative **10a**

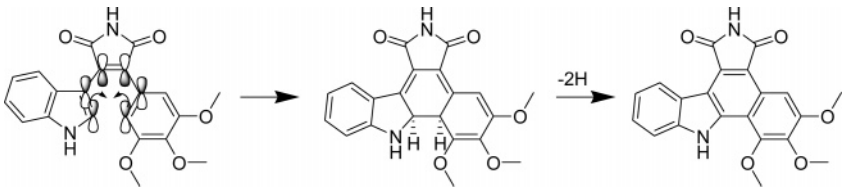

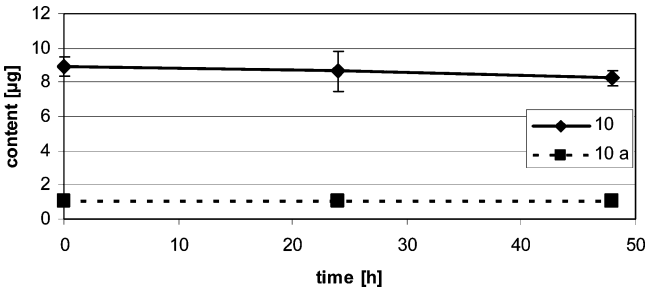

Figure 5. Content of compounds **10** and **10a** in agarose pellets time dependently across 48 h in the chick embryo model. Each point represents the mean ± SD ($n = 9$). In the first 24 h of the experiment, 0.26 μg of **10** (0.69 nmol) and 0.02 μg of **10a** (0.05 nmol) are released and target the vasculature.

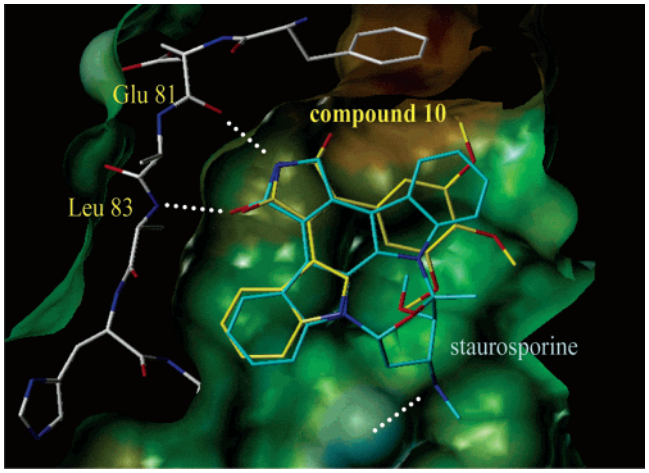

Figure 6. Crystallographically determined binding mode of staurosporine (blue) at the ATP-binding site of CDK2 and modeled binding mode of compound **10** (yellow). Key residues and hydrogen bonds are labeled.

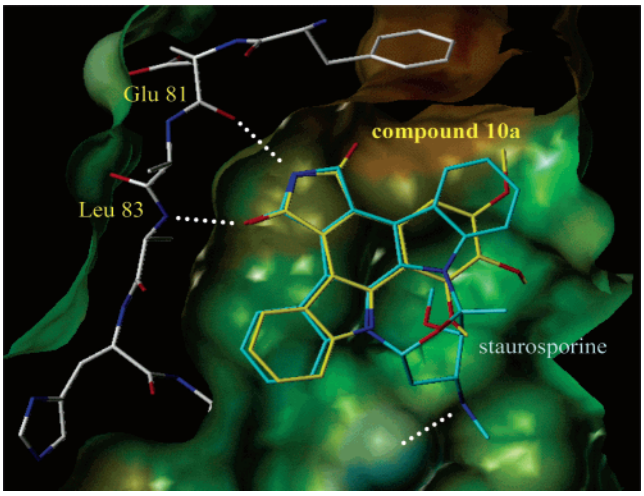

Figure 7. Crystallographically determined binding mode of staurosporine (blue) at the ATP-binding site of CDK2 and modeled binding mode of compound **10a** (yellow). Key residues and hydrogen bonds are labeled.

Since staurosporine-related diarylmaleimides have been reported to show inhibitory activity to PKC,[17] several isozymes of the PKC family (PKC-α, -γ, -ϵ, and -ι) were also included. Furthermore, members of growth factor receptor tyrosine kinases (EGF-R, ERBB2, TIE2, and VEGF-R2) were added to the panel because in particular compound **10** was a strong inhibitor of in vivo angiogenesis in the chick embryo model. The results of screening all compounds at 10 μM for inhibitory activity in the kinase panel are summarized in Table 4 (for the profile at 100 μM, see Supporting Information). The testing showed a differential inhibitory profile. Compounds **6**−**9**, **15**, **19**, and **21** have no significant inhibitory potency against any of the 12 protein kinases at 1×10^{-4} M. None of the compounds inhibited all kinases to nearly full extent at 1×10^{-4} M. Compound **18** inhibits CDK4 (87%) and CDK6 (89%), while **20** inhibits especially CDK4 (95%), CDK6 (92%), and PKC-α (93%). Compounds **10** and **10a**, used in the molecular modeling studies at CDK2, were indeed found at 10 μM to inhibit this enzyme to 42% and 41%, respectively. These results support the modeled binding mode. Remarkable inhibitory activity for compounds **10** (100%), **14** (100%), **17** (95%), and **17a** (98%) especially at the VEGF-R2 kinase (with selectivity over the other kinases) can be detected. The inhibition of VEGF-R2 of **10** and **14** matches the in vivo inhibition of angiogenesis in the chick embryo model mostly (Table 2). However, VEGF-R2 was reported to be involved in the early growth of blood vessels in the avian embryo,[34] triggering a progressive change in the branching pattern in the subsequent development stages resulting in a stable vascular architecture. [35] VEGFs are key mediators of angiogenesis and interact with cell surface receptors, in humans KDR (kinase domain-containing receptor or VEGFR-2) and Flt-1 (fms-like tyrosine kinase or VEGFR-1), expressed almost exclusively on vascular endothelial cells. [36] A third homologous receptor, VEGF-R3 (Flt-4), is constitutively expressed on adult lymphatic endothelial cells and supports lymphangiogenesis. [37] By binding to VEGFR-2/KDR, VEGFs mainly exert their mitogenic, chemotactic, and vascular permeabilizing effects on vasculature. [38] Concerning the role of VEGF-R2/KDR as an important factor in the process of angiogenesis,[39] it is possible that the inhibition of vessel growth in the in vivo model is caused by these compounds.

To evaluate the full potency against KDR tyrosine kinase and to study SAR, we decided to determine the IC_{50} values of seven selected compounds structurally related to **10** in a KDR in vitro kinase assay (Table 5).

Compound **10** was found to possess remarkable activity against this kinase showing an IC_{50} of 2.5 nM. Based on the data, SAR can be deduced by comparing **10** to the analogues. Compound **14** bearing only two methoxy groups at the phenyl system is 10^2-fold less potent than **10** indicating that all three methoxy groups contribute to the full activity. Since the pyrrole system (**11**) instead of the indole and both 5′-methoxy (**16**) and 1′-methyl substitution (**17**) of the indole system decrease activity, the unsubstituted indole moiety can be considered optimal. Particulary with regard to the indole nitrogen, investigations of Davis et al. on PKC activity of a series of similar 3-phenyl-4-indolylmaleimides derived from the structural lead staurosporine can be discussed: SAR in their work revealed that methylation at the indole nitrogen increased activity.[17] Furthermore, they found that any substituent different from hydrogen at position 4 of the phenyl system decreases activity. However, with regard to the different architecture of the ATP-binding pocket of KDR and PKC, slight structural differences of the compounds can be essential for activity and selectivity. To understand the molecular interactions, determination of the X-ray structure of **10** in complex with KDR and evaluation of the binding mode would be of interest.

Focusing on the indole in **10** adherent at the 3′-position, the analogue **21** bearing the indole moiety at the 2′-position can be compared. Interestingly, **21** showed no inhibitory activity at 10 μM in the kinase assay (Table 4) but was determined to be significantly antiangiogenic in the chick embryo assay (71.1%

Table 4. Results of All Compounds (at 10 μM) in All Kinase Assays[a]

compd	CDK2/ cycE	CDK1/ cycB	CDK4/ cycD1	CDK6/ cycD1	PKC-α	PKC-γ	PKC-ϵ	PKC-ι	EGFR	ERBB2	TIE2	VEGF-R2
2	80	103	101	70	61	76	73	103	99	99	101	19
4	83	100	113	79	90	88	108	97	109	78	108	45
5	76	102	100	69	79	83	94	99	108	92	103	55
6	87	99	108	89	85	93	105	94	103	87	100	86
7	87	87	112	81	86	89	127	102	122	85	101	94
8	79	100	88	53	82	89	98	97	106	100	99	81
9	90	108	126	96	94	98	98	95	106	88	109	100
10	58	86	54	34	29	55	33	81	83	94	14	**0**
10a	59	80	41	37	54	75	85	78	98	102	81	16
11	88	99	80	80	62	99	62	92	105	91	116	17
12	75	92	65	32	63	73	94	95	80	64	51	21
12a	80	87	75	73	90	106	107	98	86	101	136	45
13	101	101	76	47	95	83	83	77	99	93	93	17
14	93	96	105	77	65	80	77	79	90	81	65	**0**
15	103	102	115	92	94	105	98	84	107	101	108	83
16	88	105	121	96	79	99	82	85	105	97	79	**4**
16a	94	96	106	92	104	114	111	85	97	84	61	31
17	53	77	37	26	28	65	41	93	93	89	51	**5**
17a	42	43	37	25	83	94	101	80	67	60	32	**2**
18	31	48	13	11	39	65	39	78	95	92	45	16
19	90	96	126	95	97	97	100	81	72	86	119	97
20	43	30	**5**	**8**	**7**	45	21	77	102	77	71	26
21	96	97	114	95	81	101	83	83	87	88	103	89

[a] The data are presented as residual activity- in percent related to the 100% controls. Spots with residual activity <10 % are indicated with bold typeface.

Table 5. VEGF-R2 Kinase Activity of Selected Maleimides

compd	VEGF-R2 IC_{50} [μM]
10	2.5×10^{-9}
10a	6.2×10^{-8}
11	2.5×10^{-6}
14	4.3×10^{-7}
16	9.3×10^{-7}
17	6.0×10^{-7}
17a	6.4×10^{-7}

inhibition of vessel growth, Table 2). These results point to another biological target, possibly the inhibition of another kinase involved in the angiogenic process not investigated in the profile. Advanced studies of selectivity with a broad spectrum of kinases are under work. Furthermore, since related bisindolylmaleimides have been reported to be promiscuous inhibitors,[40] investigations on diverse non-kinase enzymes will answer the question of specificity in particular of compound **10**.

The carbazole derivative **10a** is about 10-fold less potent than the analogue 3,4-diarylmaleimide **10**. This fact can possibly be explained by the rigid formation caused by the carbazole. Due to the flexibility of **10**, the slightly rotated orientation of the aromatic systems maybe better fit to the binding pocket as shown in the molecular modeling studies (Figures 6 and 7). Interestingly, although **10a** was found to be active at KDR with an IC_{50} of 62 nM, no significant antiangiogenic effect can be detected in the chick embryo assay (Table 3). This was correlated to the slight solubility in the in vivo system (as discussed above). In contrast, compound **10** was shown to be bioavailable in the chick embryo model and subsequently reach the molecular target in the developing vasculature. Furthermore, these findings punctuate the physiological relevance of the chick embryo assay as a useful angiogenesis model.

Conclusions

We have synthesized a new analogue of combretastatin A-4 bearing 2,3-diarylmaleimide as a core structure (compound **2**). This compound exhibits an IC_{50} of 7.6 μM in the in vitro tubulin polymerization assay and significantly reduced angiogenesis in the in vivo chick embryo model. Furthermore, molecular modeling studies suggest a plausible binding mode of **10** at the ATP-binding site of the model kinase CDK2. Motivated by these results, a small library of 2,3-diarylmaleimides was tested in a panel of 12 selected protein kinases. This profile revealed highly potent VEGF-R2 tyrosine kinase inhibitors without the expected antitubulin activity. In particular, compound **10** possesses remarkable potency against VEGF-R2/KDR showing an IC_{50} of 2.5 nM. SAR for the isolated enzyme and equivalent anti-angiogenic activity are presented. Considering the high in vitro potency and also being bioavailable in the in vivo chick embryo assay with marked activity, certain 2,3-diarylmaleimides may have potential for clinical development as antiangiogenic drugs.

Experimental Section

Chemistry. Infrared spectra were recorded on a Perkin-Elmer 1310 infrared spectrophotometer. ^{1}H (300 MHz, digital resolution 0.3768 Hz) and ^{13}C (75 MHz, digital resolution 1.1299 Hz) NMR were recorded on a Bruker AC 300; the data are reported as follows: chemical shift in ppm from Me_4Si as external standard, multiplicity, and coupling constant (Hz). Electron impact (EI) mass spectra were recorded on a Varian MAT 311A (70 eV) and field-desorption (FD) mass spectra on a MAT-95 (Finnigan). For clarity, only the highest measured signal is given for FD mass spectra. Elemental analyses were performed on an elemental analyzer Carlo Erba Strumentazione model 1106. Combustion analyses agreed with the calculated data within ±0.4 unless otherwise stated. Melting points/decomposition temperatures were determined on a Büchi apparatus according to Dr. Tottoli and are uncorrected. X-ray structure determination was performed on a CAD4-Enraf-Nonius using Cu Kα radiation with graphite monochromator. Where appropriate, column chromatography was performed for crude precursors with Merck silica gel 60 (0.063−0.200 mm) or Acros organics silica gel (0.060−0.200 mm; pore diameter ca. 60 nm). Column chromatography for test compounds was performed using a MPLC system B-680 (Büchi) with Merck silica gel 60 (0.015−0.040 mm). The progress of the reactions was monitored by thin-layer chromatography (TLC) performed with Merck silica gel 60 F-245 plates. Where necessary, reactions were carried out in a nitrogen atmosphere using 4 Å molecular sieves. All reagents and solvents were obtained from commercial sources and used as received (THF was used after distillation over potassium/benzophenone). Reagents were purchased from Sigma-Aldrich Chemie,

Steinheim, Germany, Lancaster Synthesis, Mühlheim, Germany, or Acros, Nidderau, Germany.

3-Methylsulfonyl-4-methoxyphenylmethylglyoxalate (1) Friedel−Crafts-type Acylation. To a stirred mixture of 7.0 g (52 mmol) of $AlCl_3$ in CH_2Cl_2 at 0 °C, 7.0 g (57 mmol) of methylglyoxalate acid chloride was added dropwise. After the mixture had been stirred for 30 min, 10.0 g (50 mmol) of 1-methoxy-2-methylsulfonyloxybenzol (mesylguajacol) was added slowly. The mixture was stirred overnight at room temperature. After being quenched with ice, the organic layer was washed with water and brine. The organic phase was dried over Na_2SO_4 and concentrated to give the crude product as a brown oil. The oil was purified by silica gel column chromatography using ethyl acetate/hexanes 1/1, yielding the product as a light yellow oil, which was dried to give 4.43 g (31%) of yellowish crystals of **1** (slow crystallization). Mp = 70 °C.

General Procedure for the Preparation of Diarylmaleimides (Modified from ref 19). A stirred solution of the arylacetamide (1 equiv) and arylmethyl- or arylethylglyoxylate (2−4 equiv) in dry THF containing 15 g of molecular sieves (4 Å) was cooled to 0 °C under nitrogen. At this temperature, 1.0 M KOBu^t in ^{t}BuOH (3.0 equiv) was added via septum, and the mixture was allowed to warm to room temperature. After being stirred overnight, the reaction was again cooled to 0 °C and quenched with saturated NH_4Cl solution. The residue was filtered and extracted with ethyl acetate, and the organic phase was dried over Na_2SO_4, then concentrated and purified by column chromatography.

3-(3,4,5-Trimethoxyphenyl)-4-(3-hydroxy-4-methoxyphenyl)-1*H*-pyrrole-2,5-dione (2). The general procedure was followed using **1** (1.50 g, 5.2 mmol), 3,4,5-trimethoxyphenylacetamide (1.13 g, 5.02 mmol), and 1.0 M KOBu^t (20 mL, 20.0 mmol). Purification was achieved by column chromatography (ethyl acetate/hexanes 1/1) to yield **2** (0.85 g, 44%) as a yellow solid. Mp = 234 °C. EI-MS (*m*/*z*): 385.1 (M^+). Anal. ($C_{20}H_{19}NO_7$) C, H, N.

Structure of **2** was proven by X-ray analysis showing the compound to have the desired 3′-hydroxy and 4′-methoxy substitution pattern, as does the natural template CA-4 (Figure 2). X-ray analysis: CAD4 Enraf Nonius, Cu Kα, SIR-92, SHELXL-97. Further details of the crystal structure analysis are available in ref 41.

4-Methoxyphenylethylglyoxylate (3). For Grignard reagent, 0.49 g (20 mmol) of magnesium was stirred in diethyl ether, and 3.74 g (20 mmol) of 4-bromanisol was added. Diethyloxalate (7.5 g, 50 mmol) in diethyl ether was cooled to −78 °C and stirred mechanically while the Grignard-reagent was added slowly (color changes to yellow-brown). The reaction was allowed to warm to room temperature, NH_4Cl solution was added, and the organic layer was separated and dried over Na_2SO_4. The organic phase was concentrated under vacuum to afford a red oil, which was purified by column chromatography (ethyl acetate/hexanes 3/7) to yield **3** (2.5 g, 60%) as a yellow oil. EI-MS (*m*/*z*): 208.7 (M^+).

3-(4-Methoxyphenyl)-4-(3,4,5-trimethoxyphenyl)-1*H*-pyrrole-2,5-dione (4). The general procedure was followed using **3** (0.80 g, 3.84 mmol), 3,4,5-trimethoxyphenylacetamide (0.68 g, 3.02 mmol), and 1.0 M KOBu^t (8 mL, 8.0 mmol). Purification was achieved by column chromatography (ethyl acetate/hexanes 1/1) to yield **4** (0.79 g, 71%) as yellow crystals. Mp = 201 °C. FD-MS (*m*/*z*): 370.3 ($M^+ + 1$). Anal. ($C_{20}H_{19}NO_6$) C, H, N.

3-(3,4,5-Trimethoxyphenyl)-4-phenyl-1*H*-pyrrole-2,5-dione (5). The general procedure was followed using phenylethylglyoxylate (1.5 g, 8.42 mmol), 3,4,5-trimethoxyphenylacetamide (1.5 g, 6.66 mmol), and 1.0 M KOBu^t (20 mL, 20.0 mmol). Purification was achieved by column chromatography (ethyl acetate/hexanes 3/7) to yield **5** (0.72 g, 32%) as yellow crystals. Mp = 212 °C. EI-MS (*m*/*z*): 338.4 ($M^+ - 1$). Anal. ($C_{19}H_{17}NO_5$) C, H, N.

3-(3,4-Dimethoxyphenyl)-4-phenyl-1*H*-pyrrole-2,5-dione (6). The general procedure was followed using phenylethylglyoxylate (1.0 g, 5.61 mmol), 3,4-dimethoxyphenylacetamide (0.5 g, 2.56 mmol), and 1.0 M KOBu^t (10 mL, 10.0 mmol). Purification was achieved by column chromatography (ethyl acetate/hexanes 3/7) to yield **6** (0.41 g, 52%) as yellow crystals. Mp = 202 °C. EI-MS (*m*/*z*): 309.2 (M^+). Anal. ($C_{18}H_{15}NO_4$) C, H, N.

3-(4-Methoxyphenyl)-4-phenyl-1*H*-pyrrole-2,5-dione (7). The general procedure was followed using phenylethylglyoxylate (2.25 g, 12.63 mmol), 4-methoxyphenylacetamide (1.65 g, 10.0 mmol), and 1.0 M KOBu^t (30 mL, 30.0 mmol). Purification was achieved by column chromatography (ethyl acetate/hexanes 3/7) to yield **7** (1.58 g, 57%) as bright yellow crystals. Mp = 215 °C. EI-MS (*m*/*z*): 279.5 (M^+). Anal. ($C_{17}H_{13}NO_3$) C, H, N.

3,4-Diphenyl-1*H*-pyrrole-2,5-dione (8). The general procedure was followed using phenylethylglyoxylate (3.60 g, 20.20 mmol), phenylacetamide (1.35 g, 10.0 mmol), and 1.0 M KOBu^t (30 mL, 30.0 mmol). Purification was achieved by column chromatography (ethyl acetate/hexanes 8.5/1.5) to yield **8** (2.13 g, 86%) as bright yellow crystals. Mp = 213 °C. EI-MS (*m*/*z*): 249.5 (M^+). Anal. ($C_{16}H_{11}NO_2$) C, H, N.

3,4-Di-(4-methoxyphenyl)-1*H*-pyrrole-2,5-dione (9). The general procedure was followed using **3** (4.0 g, 19.20 mmol), 4-methoxyphenylacetamide (1.65 g, 10.0 mmol), and 1.0 M KOBu^t (25 mL, 25.0 mmol). Purification was achieved by column chromatography (ethyl acetate/hexanes 7/3) to yield **9** (1.75 g, 57%) as yellow crystals. Mp = 240 °C. EI-MS (*m*/*z*): 309.2 (M^+). Anal. ($C_{18}H_{15}NO_4$) C, H, N.

3-(Indole-3-yl)-4-(3,4,5-trimethoxyphenyl)-1*H*-pyrrole-2,5-dione (10). The general procedure was followed using indole-3-ethylglyoxylate (1.6 g, 7.38 mmol), 3,4,5-trimethoxyphenylacetamide (1.2 g, 5.33 mmol), and 1.0 M KOBu^t (20 mL, 20.0 mmol). Purification was achieved by column chromatography (ethyl acetate/hexanes 1/1) to yield **10** (1.08 g, 54%) as yellow crystals. Mp = 227 °C. EI-MS (*m*/*z*): 378.8 (M^+). Anal. ($C_{21}H_{18}N_2O_5$) C, H, N.

5,6,7-Trimethoxy-1,2,3,8-tetrahydro-benzo[*a*]pyrrolo[3,4-*c*]-carbazol-1,3-dione (10a). The product was isolated by column chromatography (ethyl acetate/hexanes 4/6) from reaction mixture **10** as bright yellow crystals (151 mg, 8%). Mp = 272 °C. EI-MS (*m*/*z*): 376.7 (M^+). Anal. ($C_{21}H_{16}N_2O_5$) C, H, N.

X-ray Crystal Structure Determination of 10 and 10a. Structures of **10**[42] and **10a**[43] have been proven by X-ray analysis (Figure 3). X-ray analysis: CAD4 Enraf Nonius, Cu Kα, SIR-92, SHELXL-97. Further details of the crystal structure analysis are available in the references.

3-(1*H*-Pyrrole-3-yl)-4-(3,4,5-trimethoxyphenyl)-1*H*-pyrrole-2,5-dione (11). The general procedure was followed using 1*H*-pyrrole-3-ethylglyoxylate (0.5 g, 2.99 mmol), 3,4,5-trimethoxyphenylacetamide (0.58 g, 2.58 mmol), and 1.0 M KOBu^t (10 mL, 10.0 mmol). Purification was achieved by column chromatography (ethyl acetate/hexanes 1/1) to yield **11** (1.08 g, 54%) as red crystals. Mp = 223 °C. EI-MS (*m*/*z*): 328.1 (M^+). Anal. ($C_{17}H_{16}N_2O_5$) calcd C 62.21, H 4.88, N 8.53; found C 61.82, H 4.32, N 8.10.

3-(Indole-3-yl)-4-phenyl-1*H*-pyrrole-2,5-dione (12). The general procedure was followed using indole-3-ethylglyoxylate (1.9 g, 10.26 mmol), phenylacetamide (3.6 g, 20.2 mmol), and 1.0 M KOBu^t (10 mL, 10.0 mmol). Purification was achieved by column chromatography (ethyl acetate/hexanes 2/8) to yield **12** (0.73 g, 25%) as yellow crystals. Mp = 240 °C. FD-MS (*m*/*z*): 289.8 ($M^+ + 1$). Anal. ($C_{18}H_{12}N_2O_2$) calcd C 74.99, H 4.20, N 9.72; found C 74.38, H 4.47, N 9.71.

1,2,3,8-Tetrahydro-benzo[*a*]pyrrolo[3,4-*c*]carbazole-1,3-dione (12a). The product was isolated by column chromatography (ethyl acetate/hexanes 2/8) from reaction mixture **12** as bright yellow crystals (86 mg, 3%). Mp > 280 °C. FD-MS (*m*/*z*): 387.6 ($M^+ + 1$). Anal. ($C_{18}H_{10}N_2O_2$) calcd C 75.32, H 3.52, N 9.79; found C 75.84, H 3.63, N 9.86.

3-(Indole-3-yl)-4-(4-methoxyphenyl)-1*H*-pyrrole-2,5-dione (13). The general procedure was followed using indole-3-ethylglyoxylate (1.17 g, 5.37 mmol), 4-methoxyphenylacetamide (0.85 g, 5.11 mmol), and 1.0 M KOBu^t (10 mL, 10.0 mmol). Purification was achieved by column chromatography (ethyl acetate/hexanes 4/6) to yield **13** (0.59 g, 36%) as yellow crystals. Mp = 220 °C. EI-MS (*m*/*z*): 318.3 (M^+). Anal. ($C_{18}H_{12}N_2O_2$) C, H, N.

3-(Indole-3-yl)-4-(3,4-dimethoxyphenyl)-1*H*-pyrrole-2,5-dione (14). The general procedure was followed using indole-3-ethylglyoxylate (0.86 g, 3.94 mmol), 3,4-dimethoxyphenylacetamide (0.70 g, 3.59 mmol), and 1.0 M KOBu^t (10 mL, 10.0 mmol).

Purification was achieved by column chromatography (ethyl acetate/hexanes 1/1) to yield **14** (0.51 g, 41%) as yellow crystals. Mp = 210 °C. EI-MS (*m/z*): 348.0 (M^+). Anal. ($C_{20}H_{16}N_2O_4$) C, H, N.

3-(Indole-3-yl)-4-(4-chlorophenyl)-1*H*-pyrrole-2,5-dione (15). The general procedure was followed using indole-3-ethylglyoxylate (1.07 g, 4.92 mmol), 4-chlorophenylacetamide (1.90 g, 5.31 mmol), and 1.0 M $KOBu^t$ (10 mL, 10.0 mmol). Purification was achieved by column chromatography (ethyl acetate/hexanes 2/8) to yield **15** (0.76 g, 45%) as yellow crystals. Mp = 275 °C. EI-MS (*m/z*): 323.5 (M^+). Anal. ($C_{18}H_{11}ClN_2O_2$) C, H, N.

3-(5-Methoxyindole-3-yl)-4-(3,4,5-trimethoxyphenyl)-1*H*-pyrrole-2,5-dione (16). The general procedure was followed using 5-methoxyindole-3-ethylglyoxylate (1.5 g, 6.07 mmol), 3,4,5-trimethoxyphenylacetamide (1.2 g, 5.33 mmol), and 1.0 M $KOBu^t$ (10 mL, 10.0 mmol). Purification was achieved by column chromatography (ethyl acetate/hexanes 4/6) to yield **16** (1.72 g, 70%) as red crystals. Mp = 268 °C. FD-MS (*m/z*): 410.1 (M^+ + 1), 408.1 (M^+). Anal. ($C_{22}H_{20}N_2O_6$) C, H, N.

11-Methoxy-5,6,7-trimethoxy-1,2,3,8-tetrahydro-benzo[*a*]-pyrrolo[3,4-*c*]carbazol-1,3-dione (16a). The product was isolated by column chromatography (ethyl acetate/hexanes 4/6) from reaction mixture **16** as red crystals (440 mg, 18%). Mp = 290 °C. FD-MS (*m/z*): 406.0 (M^+). Anal. ($C_{22}H_{18}N_2O_6$) C, H, N.

3-(1-Methylindole-3-yl)-4-(3,4,5-trimethoxyphenyl)-1*H*-pyrrole-2,5-dione (17). The general procedure was followed using 1-methylindole-3-methylglyoxylate (0.65 g, 3.0 mmol), 3,4,5-trimethoxyphenylacetamide (0.69 g, 3.06 mmol), and 1.0 M $KOBu^t$ (5 mL, 5.0 mmol). Purification was achieved by column chromatography (ethyl acetate/hexanes/CH_2Cl_2 3.5/6/0.5) to yield **17** (0.74 g, 62%) as red crystals. Mp = 187 °C. EI-MS (*m/z*): 392.2 (M^+). Anal. ($C_{22}H_{20}N_2O_6$) calcd C 67.34, H 5.14, N 7.14; found C 66.94, H 5.56, N 7.01.

5,6,7-Trimethoxy-8-methyl-1,2,3,8-tetrahydro-benzo[*a*]pyrrolo-[3,4-*c*]carbazol-1,3-dione (17a). The product was isolated by column chromatography (ethyl acetate/hexanes 4/6) from reaction mixture **17** as pale red crystals (60 mg, 5%). Mp = 185 °C. FD-MS (*m/z*): 390.2 (M^+). Anal. ($C_{22}H_{18}N_2O_5$) C, H, N.

3-(2-Methylindole-3-yl)-4-(3,4,5-trimethoxyphenyl)-1*H*-pyrrole-2,5-dione (18). The general procedure was followed using 2-methylindole-3-ethylglyoxylate (1.60 g, 6.9 mmol), 3,4,5-trimethoxyphenylacetamide (1.2 g, 5.33 mmol), and 1.0 M $KOBu^t$ (20 mL, 20.0 mmol). Purification was achieved by column chromatography (ethyl acetate/hexanes 1/1) to yield **18** (0.91 g, 44%) as red crystals. Mp = 266 °C. EI-MS (*m/z*): 393.3 (M^+ + 1). Anal. ($C_{22}H_{20}N_2O_5$) calcd C 67.34, H 5.14, N 7.14; found C 67.01, H 5.57, N 6.98.

3-(2-Phenylindole-3-yl)-4-(3,4,5-trimethoxyphenyl)-1*H*-pyrrole-2,5-dione (19). The general procedure was followed using 2-phenylindole-3-ethylglyoxylate (1.25 g, 4.26 mmol), 3,4,5-trimethoxyphenylacetamide (0.82 g, 3.06 mmol), and 1.0 M $KOBu^t$ (10 mL, 10.0 mmol). Purification was achieved by column chromatography (ethyl acetate/hexanes 1/1) to yield **19** (0.82 g, 56%) as red crystals. Mp = 304 °C. EI-MS (*m/z*): 455.2 (M^+). Anal. ($C_{27}H_{22}N_2O_5$) C, H, N.

3-(Indole-3-yl)-4-(1-naphthyl)-1*H*-pyrrole-2,5-dione (20). The general procedure was followed using indole-3-ethylglyoxylate (1.61 g, 7.40 mmol), 1-naphthylacetamide (1.0 g, 5.4 mmol), and 1.0 M $KOBu^t$ (10 mL, 10.0 mmol). Purification was achieved by column chromatography (ethyl acetate/hexanes 4/6) to yield **20** (0.44 g, 25%) as yellow crystals. Mp = 212 °C. FD-MS (*m/z*): 339.8 (M^+ + 1). Anal. ($C_{20}H_{17}N_3O_5$) calcd C 78.09, H 4.17, N 8.28; found C 76.78, H 4.49, N 7.89.

3-(Indole-2-yl)-4-(3,4,5-trimethoxyphenyl)-1*H*-pyrrole-2,5-dione (21). The general procedure was followed using indole-2-ethylglyoxylate (1.0 g, 4.61 mmol), 3,4,5-trimethoxyphenylacetamide (0.8 g, 3.0 mmol), and 1.0 M $KOBu^t$ (10 mL, 10.0 mmol). Purification was achieved by column chromatography (ethyl acetate/hexanes 1/1) to yield **21** (1.12 g, 65%) as red crystals. Mp = 252 °C. EI-MS (*m/z*): 378.7 (M^+). Anal. ($C_{21}H_{18}N_2O_5$) C, H, N.

Molecular Modeling. All modeling was performed on a Silicon Graphics O2 (R10.000) workstation. For visualization and building the structures SYBYL 6.8 [44] was used. The Connolly surface was calculated using the MOLCAD module in Sybyl and colored according to the lipophilicity (from very hydrophobic to hydrophilic corresponds to brown over green to blue). [45] Compound **10** was docked into the active site of CDK2 using the FlexX docking program (1.102). [32] The FlexX scoring function [46] was applied during the placement and construction phase of the ligands and DrugScore for the final ranking. [47] The 3D coordinates of the CDK2 catalytic core in complex with staurosporine were taken from the Brookhaven Protein Databank (PDB code: 1AQ1). [48]

Chick Embryo Assay as in Vivo Angiogenesis Model. The assay was basically performed according to the procedure in ref 49. Test compounds were dissolved in DMSO and used as stock solution. For the preparation of agarose pellets, the stock solution was mixed with 2% agarose solution at 80 °C, and 10 μL pellets were produced (final content 5−100 μg).

Fertilized chicken eggs (White leghorn, Freddy's Hühnerhof GmbH & Co. KG, Mainz, Germany) were incubated at 37.5 °C and 62% relative humidity in an automatically turning egg incubator (Ehret). After 70 h of incubation and removal of 8 mL of albumen, a window was opened in the shell to uncover the developing germination layer. The window was sealed with transparent tape; the eggs were returned to the incubator and stored at 90% relative humidity without turning. At 75-h incubation time, the angiogenic experiment was initiated (start time 0 h) and 15 agarose pellets were placed on the area vasculosa preparations. After 24 h, images of the control and sample-treated areas were captured. Images were digitized via Leica QWinTM-Software, and the angiogenic response was measured using the automatic image analysis system programmed in a routine. Captured and digitized images were analyzed for total, major (capillaries with a diameter of more than 50 μm), and minor blood vessel areas using the customized image analysis software Leica QWinTM (Leica Microsystems Bensheim, Germany). Calculated data were sent automatically via dynamic data exchange to an Excel table and processed statistically. An anti-angiogenic response due to agent-treated samples was considered positive if the mean of minor blood vessel area showed >20% inhibition compared to control samples. Differences between treated and control samples were evaluated using Student's *t*-test.

Tubulin Polymerization Assay. The antimitotic activity of the compounds was determined using a slightly modified version of the turbidimetric tubulin assembly in vitro assay described by Gaskin et al.[50]

In this assay, the assembly of microtubule protein isolated from porcine brain (method according to Shelanski et al.[50a] is monitored in vitro in the presence of effectors. The principle is based on the fact that microtubules increase the turbidity of the test solution compared to unpolymerized tubulin dimers. The degree of assembly is measured by detecting the change in absorbance of the test solution compared to a control.

The measurements were performed at 360 nm with a Uvikon 930 UV spectrophotometer (Kontron Instruments) equipped with a multicell holder connected to a thermostat. The influence of the test substances on tubulin assembly (protein concentration 1 mg/mL) was determined by comparing the change of absorption to a control without effectors. Assembly was performed for 20 min in a PIPES (piperazine-1,4-bis-(2-ethanesulfonic acid)) buffer containing 10 mM GTP at pH 6.8 and a temperature of 37 °C. To exclude protein denaturation and to check reversibilty of assembly, the measurement was continued for additional 20 min while decreasing the temperature to 4 °C, which should shift turbidity to the pre-assembly level.

Selectivity Profiling of Compounds in Two Concentrations Using 12 Protein Kinases. Recombinant Protein Kinases. The inhibitory profile of compounds was determined using the following 12 protein kinases: CDK1/cyclinB, CDK2/cyclinE, CDK4/cyclinD1, CDK6/cyclinD1, PKC-α, PKC-γ, PKC-ϵ, PKC-ι, EGF-R, ERBB2, TIE2, and VEGF-R2.

All protein kinases were expressed in Sf9 insect cells as recombinat GST fusion proteins or His-tagged proteins by means of the baculovirus expression system. Except for PKC-α (mouse),

PKC-ϵ (mouse), and PKC-γ (rat), human cDNAs were used for the expression of the protein kinases. Kinases were purified by affinity chromatography using either GSH-agarose (Sigma) or Ni−NTH-agarose (Qiagen). The purity and identity of each kinase was checked by SDS−PAGE/silver staining and by Western blot analysis with specific antibodies.

Protein Kinase Assay. A proprietary protein kinase assay (^{33}PanQinase Activity Assay) was used for measuring the kinase activity of the 12 protein kinases. All kinase assays were performed in 96-well FlashPlates from Perkin-Elmer/NEN (Boston, MA) in a 50 μL reaction volume.

The assay for all enzymes (except for the PKC assay, see below) contained 60 mM HEPES−NaOH, pH 7.5, 3 mM $MgCl_2$, 3mM $MnCl_2$, 3 μM sodium orthovanadate, 1.2 mM DTT, 50 μg/mL PEG_{20000}, 1 μM [γ-^{33}P]-ATP (approximately 5×10^5 cpm per well), recombinant protein kinase (50−400 ng), and depending on the kinase, the following substrate proteins: Rb-CTF (CDK1, CDK4, CDK6), poly(Glu,Tyr)4:1 (EGF-R, ERBB2, TIE2, VEGF-R2), and histone H1 (CDK2).

The PKC assay contained 60 mM HEPES−NaOH, pH 7.5, 1 mM EDTA, 1.25 mM EGTA, 5 mM $MgCl_2$, 1.32 mM $CaCl_2$, 5 μg/mL phosphatidylserine, 1μg/mL 1,2-dioleyl glycerol, 1.2 mM DTT, 50 μg/mL PEG_{20000}, 1 μM [γ-^{33}P]-ATP (approximately 5×10^5 cpm per well), recombinant protein kinase (20−100 ng), and histone H1 as substrate.

The compounds were tested at concentrations of 10 and 100 μM in singlicate. The final DMSO concentration in the assay was 1%.

The reaction cocktails were incubated at 30 °C for 80 min. The reaction was stopped with 50 μL of 2% (v/v) H_3PO_4, and plates were aspirated and washed two times with 200 μL of 0.9% (w/v) NaCl. Incorporation of $^{33}P_i$ was determined with a microplate scintillation counter (Microbeta Trilux, Wallac). All assays were performed with a BeckmanCoulter/Sagian robotic system.

For each compound, inhibition was calculated as percentage relative to control values without test compound.

Acknowledgment. Financial support by the Ministerium für Umwelt und Forsten/Mainz and the Fonds der Chemischen Industrie, Germany, is gratefully acknowledged.

Supporting Information Available: MS, NMR, IR-data, and selectivity profiling for compounds at 100 μM using 12 kinases. This material is available free of charge via the Internet at http://pubs.acs.org.

References

(1) Carmeliet, P.; Jain, R. K. Angiogenesis in cancer and other diseases. *Nature* **2000**, 407, 249−257.
(2) Fan, T. D.; Brem, S. In *Angiosuppression. The search for new anticancer drugs*; Waring, M. J., Ponder, B., Eds.; Kluwer Academic Press: Dordrecht, The Netherlands, 1992; pp 185−229.
(3) Yancopoulus, G. D.; Davis, S.; Gale, N. W.; Rudge, J. S.; Wiegand, S. J.; Holash, J. Vascular-specific growth factors and blood vessel formation. *Nature* **2000**, *407*, 242−248.
(4) Tozer, G. M.; Prise, V. E.; Wilson, J.; Locke, R. J.; Vojnovic, B.; Stratford, M. R. L.; Dennis, M. F.; Chaplin, D. J. Combretastatin A-4 phosphate as a tumor vascular-targeting agent: early effects in tumors and normal tissues. *Cancer Res.* **1999**, *59*, 1626−1634.
(5) Jordan, A.; Hadfield, J. A.; Lawrence, N. J.; McGown, A. T. Tubulin as a target for anticancer drugs: agents which interact with the mitotic spindle. *Med. Res. Rev.* **1998**, *18*, 259−296.
(6) Flynn, B. L.; Hamel, E.; Jung, M. K. One-pot synthesis of benzo-[*b*]furan and indole inhibitors of tubulin polymerization. *J. Med. Chem.* **2002**, *45*, 2670−2673.
(7) Bibby, M. C. Combretastatin anticancer drugs. *Drugs Future* **2002**, *27* (5), 475−480.
(8) Bailly, C.; Bal, C.; Barbier, P.; Combes, P.; Finet, J.-P.; Hildebrand, M.-P.; Peyrot, V.; Wattez, N. Synthesis and biological evaluation of 4-Arylcoumarin analogues of combretastatins. *J. Med. Chem.* **2003**, *46* (25), 5437−5444.
(9) Woods, J. A.; Hadfield, J. A.; Pettit, G. R.; Fox, B. W.; McGown, A. T. The interaction with tubulin of a series of stilbenes based on combretastatin A-4. *Br. J. Cancer* **1995**, *71*, 705−711.
(10) Gaukroger, K.; Hadfield, J. A.; Hepworth, L. A.; Lawrence, N. J.; McGown, A. T. Novel syntheses of cis and trans isomers of combretastatin A-4. *J. Org. Chem.* **2001**, *66*, 8135−8138.
(11) Wang, L.; Woods, K. W.; Li, Q.; Barr, K. J.; McCroskey, R. W.; Hannick, S. M.; Gherke, L.; Credo, B. R.; Hui, Y. H.; Marsh, K.; Warner, R.; Lee, J. Y.; Zielinski-Mozng, N.; Frost, D.; Rosenberg, S. H.; Sham, H. L. Potent, orally active Heterocycle-based CA-4 analogues. Synthesis, Structure−Activity Relationship, Pharmacokinetics, and in vivo antitumor activity evaluation. *J. Med. Chem.* **2002**, *45*, 1697−1711.
(12) Shirai, R.; Takayama, H.; Nishikawa, A.; Koiso, Y.; Hashimoto, Y. Asymmetric synthesis of antimitotic combretadioxolane with potent antitumor activity against multi-drug resistant cells. *Bioorg. Med. Chem. Lett.* **1998**, *8*, 1997−2000.
(13) Medarde, M.; Ramos, A. C.; Pelaez, R.; López, J. L.; Grávalos, D. G.; San Feliciano, A. Synthesis and pharmacological activity of diarylindole derivatives. Cytotoxic agents based on combretastatins. *Bioorg. Med. Chem. Lett.* **1999**, *9*, 2303.
(14) Simoni, D.; Grisolia, G.; Giannini, G.; Roberti, M.; Rondanin, R.; Piccagli, L.; Baruchello, R.; Rossi, M.; Romagnoli, R.; Invidiata, F. P.; Grimaudo, S.; Jung, M. K.; Hamel, E.; Gebbia, N.; Crosta, L.; Abbadessa, V.; Di Cristina, A.; Dusonchet, L.; Meli, M.; Tolomeo, M. Heterocyclic and Phenyl Double-Bond-Locked Combretastatin Analogues Possessing Potent Apoptosis-Inducing Activity in HL60 and in MDR Cell Lines. *J. Med. Chem.* **2005**, *48* (3), 723−736.
(15) Moreau, P.; Anizon, F.; Sancelme, M.; Prudhomme, M.; Bailly, C.; Carrasco, C.; Ollier, M.; Severe, D.; Riou, J. F.; Fabbro, D.; Meyer, T.; Aubertin, A. M. Syntheses and biological evaluation of indolocarbazoles, analogues of rebeccamycin, modified at the imide heterocycle. *J. Med. Chem.* **1998**, *7*, *41* (10), 1631−1640.
(16) Gray, N.; Detivaud, L.; Doering, C.; Meijer, L. ATP-site directed inhibitors of cyclin-dependent kinases. *Curr. Med. Chem.* **1999**, *6* (9), 859−875.
(17) Davis, P. D.; Hill, C. H.; Lawton, G.; Nixon, J. S.; Wilkinson, S. E.; Hurst, S. A.; Keech, E.; Turner, S. E. Inhibitors of protein kinase C. 1. 2,3-Bisarylmaleimides. *J. Med. Chem.* **1992**, *35* (1), 177−184.
(18) Zhang, H.-C.; Ye, H.; Conway, B. C.; Derian, C. K.; Addo, M. F.; Kuo, G. H.; Hecker, L. R.; Croll, J. L.; Westover, L.; Xu, J. Z.; Look, R.; Demarest, K. T.; Andrade-Gordon, P.; Damiano, B. P.; Maryanoff, B. E. 3-(7-Azaindolyl)-4-arylmaleimides as potent, selective inhibitors of glycogen synthase kinase-3. *Bioorg. Med. Chem. Lett.* **2004**, *14*, 3245−3250.
(19) (a) Faul, M. M.; Winneroski, L. L.; Krumrich, C. A. A new one Step Synthesis of maleimides by condensation of glyoxylate esters with acetamides. *Tetrahedron Lett.* **1999**, *40*, 1109−1112. (b) Faul, M. M.; Winneroski, L. L.; Krumrich, C. A. A new, efficient method for the synthesis of bisindolylmaleimides. *J. Org. Chem.* **1998**, *63*, 6053−6058.
(20) Creary, X.; Mehrsheikh-Mohammadi, M. E. Captodative rate enhancements in the methylenecyclopropane rearrangement. *J. Org. Chem.* **1986**, *51*, 2664−2668.
(21) Bensel, N.; Pevere, V.; Desmurs, J. R.; Wagner, A.; Mioskowski, C. Mesyl guajacol: a versatile intermediate for the synthesis of 5-aminomethyl guajacol and related compounds. *Tetrahedron Lett.* **2002**, *43*, 4281−4283.
(22) (a) Okauchi, T.; Itonaga, M.; Minami, T.; Owa, T.; Kitoh, K.; Yoshino, H. A general method for acylation of indoles at the 3-position with acyl chlorides in the presence of dialkylaluminium chloride. *Org. Lett.* **2000**, *2* (10), 1485−1487. (b) Ottoni, O.; Neder, A. de V. F.; Dias, A. K. B.; Cruz, R. P. A.; Aquino, L. B. Acylation of indole under Friedel−Crafts conditions- an improved method to obtain 3-Acylindoles regioselectively. *Org. Lett.* **2001**, *3* (7), 1005−1007.
(23) Zhang, Z.; Yang, Z.; Wong, H.; Zhu, J.; Meanwell, N. A.; Kadow, J. F.; Wang, T. An effective procedure for the acylation of azaindoles at C-3. *J. Org. Chem.* **2002**, *67*, 6226−6227.
(24) Bray, B. L.; Mathies, P. H.; Naef, R.; Solas, D. R.; Tidwell, T. T.; Artis, D. R.; Muchowski, J. M. *N*-(Triisopropylsilyl)pyrrole. A progenitor "par excellence" of 3-substituted pyrroles. *J. Org. Chem.* **1990**, *55*, 6317−6328.
(25) Tholander, J.; Bergman, J. Syntheses of 6,12-disubstituted 5,11-dihydroindolo[3,2-*b*]carbazoles, including 5,11-dihydroindolo[3,2-*b*]carbazole-6,12-dicarbaldehyde, an extremely efficient ligand for the TCDD (Ah) receptor. *Tetrahedron* **1999**, *55* (43), 12577−12594.
(26) Pindur, U.; Kim, Y.-S.; Mehrabani, F. Advances in indolo[2,3-a]-carbazole chemistry: design and synthesis of Protein kinase C and topoisomerase-I-inhibitors. *Curr. Med. Chem.* **1999**, *6*, 29−69.
(27) Reddy, G. M.; Chen, S.-Y.; Uang, B.-J. A facile synthesis of indolo-[2,3-a]pyrrolo[3,4-c]carbazoles via oxidative photocyclization of bisindolylmaleimides. *Synthesis* **2003**, *4*, 497−500.
(28) Harris, W.; Hill, C. H.; Keech, E.; Malsher, P. Oxidative cyclisations with palladium acetate. A short synthesis of staurosporine aglykon. *Tetrahedron Lett.* **1993**, *34* (51), 8361−8364.

(29) Noble, M. E.; Endicott, J. A.; Johnsen, L. N. *Science* **2004**, *303*, 1800−1805.
(30) Davies, T. G.; Pratt, D. J.; Endicott, J. A.; Johnson, L. N.; Noble, M. E. M. Structure-based design of cyclin-dependent kinase inhibitors. *Pharmacol. Ther.* **2002**, *93*, 125−133.
(31) Lawrie, A. M.; Noble, M. E.; Tunnah, P.; Brown, N. R.; Johnson, L. N.; Endicott, J. A. *Nat. Struct. Biol.* **1997**, *4*, 796−801.
(32) Rarey, M.; Kramer, B.; Lengauer, T.; Klebe, G. A fast flexible docking method using an incremental constructing algorithm. *J. Mol. Biol.* **1996**, *261* (3), 470−489.
(33) Sielecki, T. M.; Boylan, J. F.; Benfield, P. A.; Trainor, G. L. Cyclin-dependent kinase inhibitors: useful targets in cell cycle regulation. *J. Med. Chem.* **2000**, *43*, 1−18.
(34) Aitkenhead, M.; Christ, B.; Eichmann, A.; Feucht, M.; Wilson, D. J.; Wilting, J. Paracrine and autocrine regulation of vascular endothelial growth factor during tissue differentiation in the quail. *Dev. Dyn.***1998**, *212*, 1−13.
(35) Vico, P. G.; Kyriacos, S.; Heymans, O.; Louryan, S.; Cartilier, L. Dynamic study of the extraembryonic vascular network of the chick embryo by fractal analysis. *J. Ther. Biol.* **1998**, *195*, 525−532.
(36) Neufeld, G.; Cohen, T.; Gengrinovitch, S.; Poltorak, Z. Vascular endothelial growth factor (VEGF) and its receptors. *FASEB J.* **1999**, *13*, 9−22.
(37) Korpelainen, E. I.; Alitalo, K. Signaling angiogenesis and lymphangiogenesis. *Curr. Opin. Cell Biol.* **1998**, *10*, 159−164.
(38) Gille, H.; Kowalski, J.; Li, B.; LeCouter, J.; Moffat, B.; Zioncheck, T. F.; Pelletier, L.; Ferrara, N. Analysis of biological effects and signaling properties of Flt-1 (VEGF-R1) and KDR (VEGF-R2). *J. Biol. Chem.* **2001**, *276*, 3222−3230.
(39) Dvorak, H. F. Vascular permeability factor/vascular endothelial growth factor: a critical cytokine in tumor angiogenesis and a potential target for diagnosis and therapy. *J. Clin. Oncol.* **2002**, *20* (21), 4368−4380.
(40) McGovern, S. L.; Shoichet, B. K. Kinase inhibitors: Not just for kinases anymore. *J. Med. Chem.* **2003**, *46*, 1478−1483.
(41) Schollmeyer, D.; Peifer, C.; Dannhardt, G. 3-(3,4,5-Trimethoxyphenyl)-4-(3-hydroxy-4-methoxyphenyl)-1*H*-pyrrole-2,5-dione. *Acta Crystallogr.* **2005**, *E61*, 604−606.
(42) Peifer, C.; Schollmeyer, D.; Dannhardt, G. 3-(Indole-3-yl)-4-(3,4,5-trimethoxyphenyl)-1*H*-pyrrole-2,5-dione. *Acta Crystallogr.* **2005**, *E61*, 721−723.
(43) Peifer, C.; Schollmeyer, D.; Dannhardt, G. 5,6,7-Trimethoxy-1,2,3,8-tetrahydro-benzo[*a*]pyrrolo[3,4-*c*]carbazole-1,3-dione containing one equivalent of DMSO. *Acta Crystallogr.* **2005**, *E61*, 724−725.
(44) *SYBYL Molecular Modeling Software*, 6.8 ed., Tripos Inc.: St. Louis, MO, 1992.
(45) Waldherr-Teschner, M.; Henn, Ch.; Vollhardt, H.; Reiling, S.; Brickmann, J. Texture Mapping: a new tool for molecular graphics. *J. Mol. Graphics* **1994**, *12* (2), 89−105.
(46) Böhm, H. J. The development of a simple empirical scoring function to estimate the binding constant for a protein−ligand complex of known three-dimensional structure. *J. Comput.-Aided Mol. Des.* **1994**, *8* (3), 243−256.
(47) Gohlke, H.; Hendlich, M.; Klebe, G. Knowledge-based scoring function to predict protein−ligand interactions. *J. Mol. Biol.* **2000**, *295* (2), 337−356.
(48) Lawrie, A. M.; Noble, M. E.; Tunnah, P.; Brown, M. R.; Johnson, L. N.; Endicott, J. A. *Nat. Struct. Biol.* **1997**, *4*, 796−801.
(49) Peifer, C.; Dannhardt, G. A novel quantitative chick embryo assay as an angiogenesis model using digital image analysis. *Anticancer Res.* **2004**, *24*, 3A, 1545−1552.
(50) (a) Gaskin, F.; Cantor, C. R.; Shelanski, M. L. Turbidimetric studies of the in vitro assembly and disassembly of porcine neurotubules. *J. Mol. Biol.* **1974**, *89* (4), 737−755. (b) Shelanski, M. L.; Gaskin, F.; Cantor, C. R. Microtubule assembly in the absence of added nucleotides. *Proc. Natl. Acad. Sci. U.S.A.* **1973**, *70*, 765−768.

JM0580297